Characterization of the Human Skeletal Muscle Proteome by One-dimensional Gel Electrophoresis and HPLC-ESI-MS/MS*,S

Kurt Højlund[‡,§,¶,‖], **Zhengping Yi**[‡,¶,**,‡‡], **Hyonson Hwang**[‡,§§], **Benjamin Bowen**[‡,¶¶], **Natalie Lefort**[‡,§§], **Charles R. Flynn**[‡], **Paul Langlais**[‡,§§], **Susan T. Weintraub**[‖‖], and **Lawrence J. Mandarino**[‡,**,§§]

[‡]Center for Metabolic Biology, Arizona State University, Tempe, Arizona

[§]Diabetes Research Centre, Department of Endocrinology, Odense University Hospital, Odense, Denmark

[**]School of Life Sciences, Arizona State University, Tempe, Arizona

[§§]Department of Kinesiology, Arizona State University, Tempe, Arizona

[¶¶]Harrington Department of Bioengineering, Arizona State University, Tempe, Arizona

[‖‖]Department of Biochemistry, University of Texas Health Science Center at San Antonio, San Antonio, Texas

Abstract

Changes in protein abundance in skeletal muscle are central to a large number of metabolic and other disorders, including, and perhaps most commonly, insulin resistance. Proteomics analysis of human muscle is an important approach for gaining insight into the biochemical basis for normal and pathophysiological conditions. However, to date, the number of proteins identified by this approach has been limited, with 107 different proteins being the maximum reported so far. Using a combination of one-dimensional gel electrophoresis and high performance liquid chromatography electrospray ionization tandem mass spectrometry, we identified 954 different proteins in human vastus lateralis muscle obtained from three healthy, nonobese subjects. In addition to a large number of isoforms of contractile proteins, we detected all proteins involved in the major pathways of glucose and lipid metabolism in skeletal muscle. Mitochondrial proteins accounted for 22% of all proteins identified, including 55 subunits of the respiratory complexes I–V. Moreover, a number of enzymes involved in endocrine and metabolic signaling pathways as well as calcium homeostasis were identified. These results provide the most comprehensive characterization of the human skeletal muscle proteome to date. These data hold promise for future global assessment of quantitative changes in the muscle proteome of patients affected by disorders involving skeletal muscle.

The percutaneous muscle biopsy technique is an important tool in the diagnosis and management of human muscle disorders and has been used widely to investigate many

[‡‡]To whom correspondence should be addressed: Center for Metabolic Biology, College of Liberal Arts and Sciences, PO Box 873704, Tempe, AZ 85287–3704; Tel.: 480-727-7602; Fax: 480-727-6813; zhengping.yi@asu.edu.
[¶]These authors contributed equally to the work.

aspects of cell structure and metabolism in normal and abnormal human muscle (1, 2). There is a lack of comprehensive knowledge of the molecular basis of changes in protein expression that are part of normal physiologic adaptations, such as those that occur during exercise training or age-related sarcopenia, or pathophysiological changes associated with disease processes, including atrophy (caused by disuse, spinal cord injury, or weightlessness), ischemic damage, muscular dystrophies, and insulin resistance. Insulin resistance in skeletal muscle is a condition that is common to obesity, type 2 diabetes, and cardiovascular disease. These diseases affect 25–50 million individuals in the United States alone and many more worldwide. During the past decades, percutaneous needle biopsy of the vastus lateralis muscle has played an important role in defining the molecular abnormalities underlying insulin resistance (3–5). On the basis of such studies, an increasing number of genes and proteins in several signaling and metabolic pathways have been implicated in skeletal muscle insulin resistance (3–7). However, the majority of studies have focused on only a limited number of genes and proteins. Other investigators have used the needle muscle biopsy technique to study biochemical, histological, and molecular abnormalities in other common diseases, such as the muscular dystrophies (8).

There is a clear need for approaches capable of evaluating global changes in protein expression and modification. High throughput gene expression technologies such as cDNA microarrays are powerful tools for the study of physiological and pathological conditions with complex or multifactorial underlying mechanisms, proving useful in studies of age-related sarcopenia (9), muscle insulin resistance (10–13), muscular dystrophy (8), denervation (14), and endurance training (15). However, expression of muscle mRNA may not accurately reflect the abundance of proteins and can give no information regarding their posttranslational modifications (16, 17), indicating the need to correlate the results from global gene expression experiments and measurements of protein abundance.

Although human vastus lateralis muscle has been used in thousands of studies within the past decade, only a few proteomic studies have been conducted, combining protein separation by two-dimensional gel electrophoresis and protein identification by mass spectrometry (18–23). Previously, the most comprehensive assessment of the human vastus lateralis proteome reported only 107 different proteins (18). The high abundance of cytoskeletal and contractile proteins combined with dynamic range issues associated with the two-dimensional gel approach may be factors that have hampered studies on this topic.

The use of two orthogonal liquid chromatography steps for peptide separation prior to tandem mass spectrometry (MS/MS)[1] (24) has yielded substantial improvements in detection limits; consequently, identification of increased numbers of proteins in mammalian tissues (25, 26). Recently, two-dimensional high performance liquid chromatography electrospray ionization tandem mass spectrometry (HPLC-ESI-MS/MS) was used to analyze the proteome of human beta cells, resulting in the identification of 3365 unique proteins (27). An alternative to two-dimensional gels and two-dimensional HPLC uses separation by one-dimensional SDS-PAGE and subsequent protein identification by HPLC-ESI-MS/MS (28, 29). This approach has been shown to be comparable to two-dimensional HPLC-ESI-MS/MS with respect to the number of proteins identified (30). Moreover, it is simpler from a technological point of view and is suitable for clinical studies of small tissue samples obtained *in vivo* by biopsy.

---

[1]The abbreviations used are: FA, formic acid; ACN, acetonitrile; CID, collision-induced dissociation, OXPHOS, oxidative phosphorylation; MW, molecular weight; MS/MS, tandem mass spectrometry; HPLC, high performance liquid chromatography; ESI electrospray ionization.

In the present study, we used one-dimensional gel electrophoresis and HPLC-ESI-MS/MS to characterize the proteome of human skeletal muscle obtained using percutaneous needle biopsies of the vastus lateralis muscle in healthy volunteers. We identified 954 proteins, including all enzymes participating in the major pathways of glucose and lipid metabolism, a large number of proteins involved in mitochondrial oxidative phosphorylation and calcium homeostasis, and most isoforms of the proteins that constitute the myofibrillar apparatus. As such, the proteins identified in our analyses provide a representation of the major biological functions of skeletal muscle.

EXPERIMENTAL PROCEDURES

Subjects

The skeletal muscle samples used for the proteomics analyses in this study were obtained from three healthy, nonobese volunteers (I–III; age, 30–47 years; body mass index, 24–28 kg/m^2; percent body fat, 23–34%) with normal glucose tolerance and no family history of type 2 diabetes. The purpose, nature, and potential risks of the study were explained to the participants, and written consent was obtained before participation. The protocol was approved by the Institutional Review Board of Arizona State University.

Muscle Preparation, Electrophoresis, and Staining

A percutaneous needle biopsy of the vastus lateralis muscle was obtained under local anesthesia, and the muscle biopsy specimen was immediately blotted free of blood, frozen, and stored in liquid nitrogen until use. For protein analysis, the muscle biopsy specimens were homogenized while still frozen in an ice-cold buffer (10 μl/mg tissue) consisting of (final concentrations): 50 mM HEPES, pH 7.6, 150 mM NaCl, 20 mM sodium pyrophosphate, 20 mM -glycerophosphate, 10 mM NaF, 2 mM sodium orthovanadate, 2 mM EDTA, 1% Triton, 10% glycerol, 2 mM phenylmethylsulfonyl fluoride, 1 mM $MgCl_2$, 1 mM $CaCl_2$, 10 μg/ml leupeptin, and 10 μg/ml aprotinin. A Polytron homogenizer (Brinkman Instruments, Westbury, NY) set on maximum speed for 30 s was used for homogenization. The homogenate was cooled on ice for 20 min and then centrifuged at $10,000 \times g$ for 20 min at 4 °C; the resulting supernatant was frozen until use. Protein concentrations were determined by the method of Lowry (31). Two experiments were performed. Experiment 1: subject I, 75 μg of muscle lysate, proteins separated on a 10% SDS-polyacrylamide gel, and HPLC-MS/MS run in duplicate (Experiments 1–1 and 1–2). Experiments 2–1 and 2–2: 60 μg of muscle lysate proteins from subjects II and III, respectively, were separated on 4–20% gradient SDS-polyacrylamide gels; proteins were visualized with Coomassie blue (Sigma Chemical Co., St. Louis, MO).

In-gel Digestion

The gel lane resulting from each experiment was cut into 20–24 slices of approximately equal size. Each slice was cut into 1-mm cubes prior to digestion. The gel pieces were placed in a 0.6-ml polypropylene tube, washed with 400 μl of water, destained twice with 300 μl of 50% acetonitrile (ACN) in 40 mM NH_4HCO_3, and dehydrated with 100% ACN for 15 min. After removal of the ACN by aspiration, the gel pieces were dried in a vacuum centrifuge at 62 °C for 30 min. Trypsin (250 ng; Sigma Chemical Co.) in 30 μl of 40 mM NH_4HCO_3 was added and the samples were maintained at 4 °C for 15 min prior to the addition of 50 μl of 40 mM NH_4HCO_3. The digestion was allowed to proceed at 37 °C overnight and was terminated by the addition of 10 μl 5% formic acid (FA). After incubation at 37 °C for an additional 30 min and centrifugation for 1 min, each supernatant was transferred to a clean polypropylene tube. The extraction procedure was repeated using 80 μl of 0.5% FA, and the two extracts were combined. The sample volume was reduced to ~5 μl

by vacuum centrifugation, and 20 μl of 0.05% heptafluorobutyric acid/1% FA: 2%ACN was added.

Mass Spectrometry

HPLC-ESI-MS/MS was performed on a hybrid linear ion trap (LTQ)-Fourier Transform Ion Cyclotron Resonance mass spectrometer (LTQ FT; Thermo Fisher; San Jose, CA) fitted with a PicoView nanospray source (New Objective, Woburn, MA). The mass spectrometer was calibrated weekly according to manufacturer's instructions, achieving mass accuracy of the calibrants within 2 ppm. On-line capillary HPLC was performed using a Michrom BioResources Paradigm MS4 micro HPLC (Auburn, CA) with a PicoFrit column (New Objective; 75 μm inner diameter, packed with ProteoPep II C18 material, 300 Å). Samples were desalted using an on-line Nanotrap (Michrom BioResources) before being loaded onto the PicoFrit column. HPLC separations were accomplished with a linear gradient of 2 to 27% ACN in 0.1% FA in 70 min, a hold of 5 min at 27% ACN, followed by a step to 50% ACN, hold 5 min and then a step to 80%, hold 5 min; flow rate, 300 nl/min. A "top-10" data-dependent tandem mass spectrometry approach was utilized to identify peptides in which a full scan spectrum (survey scan) was acquired followed by collision-induced dissociation (CID) mass spectra of the 10 most abundant ions in the survey scan. The survey scan was acquired using the Fourier Transform Ion Cyclotron Resonance mass analyzer to obtain high resolution, high mass accuracy data.

Data Analysis and Bioinformatics

Tandem mass spectra were extracted from Xcalibur "RAW" files and charge states were assigned using the Extract MSN script that is a component of Xcalibur 2.0 SR2 (Thermo Fisher). Charge states and monoisotopic peak assignments were then verified using DTA-SuperCharge, part of the MS-Quant suite of software (32), before all "DTA" files from each gel lane in an experiment were combined into a single Mascot Generic format file. The fragment mass spectra were then searched against the IPI_HUMAN_v3.27 database (67,528 entries, http://www.ebi.ac.uk/IPI/) using Mascot (Matrix Science, London, United Kingdom, version 2.2). The false discovery rate was determined by selecting the option to use a "decoy" randomized search strategy that is available in Mascot, v2.2. The search parameters that were used were: 10 ppm mass tolerance for precursor ion masses and 0.5 Da for product ion masses; digestion with trypsin; a maximum of two missed tryptic cleavages; variable modifications of oxidation of methionine and phosphorylation of serine, threonine, and tyrosine. Probability assessment of peptide assignments and protein identifications were made through use of Scaffold (version Scaffold-01_06_17, Proteome Software Inc., Portland, OR). Only peptides with 95% probability were considered. Criteria for protein identification included detection of at least 2 unique identified peptides and a probability score of 95%. Proteins that contained identical peptides and could not be differentiated based on MS/MS analysis alone were grouped. Multiple isoforms of a protein were reported only if they were differentiated by at least one unique peptide with 95% probability, based on Scaffold analysis. IPI accession numbers for identified proteins were input into the UniProt database (www.pir.uniprot.org) to obtain Gene Ontology annotation.

RESULTS

Characteristics of Human Skeletal Muscle Proteome

To obtain a comprehensive proteomic characterization of the human vastus lateralis muscle, we carried out HPLC-ESI-MS/MS-based analysis of lysates of whole muscle from which proteins were first fractionated by one-dimensional gel electrophoresis. We first performed duplicate HPLC-ESI-MS/MS analyses (experiments 1–1 and 1–2) on proteins isolated from the muscle of subject I to assess the reproducibility of the approach. In these analyses, 591

and 577 proteins were identified, respectively, corresponding to a total of 668 unique proteins. There were at least two unique peptides (95% confidence) assigned to each identified protein, all with a confidence level   95% based on the Scaffold analysis. The false discovery rates as assessed by Mascot searching of a randomized database were 3.1% and 3.4%, respectively. Among these proteins, 500 were identified in both experiments 1–1 and 1–2, giving a reproducibility rate of ~75%. Data analysis showed that the three major isoforms of myosin heavy-chain (myosin 1, 2, and 7) comprised ~42% of the total spectra, indicating that the analytical space taken up by these myosin isoforms may hamper identification of other proteins that migrate similarly in SDS-polyacrylamide gels. In an attempt to minimize this, in subsequent analyses for subjects II and III, we used gradient gels (4–20%) to obtain a better separation of proteins; after separation on the gradient gels, we identified 571 and 616 proteins for subjects II and III, respectively; the proportion of spectra assigned to the 3 major myosin heavy-chain isoforms was reduced to ~32%. The false discovery rate was 5.6% and 5.2%, respectively. A total of 741 unique proteins were identified in the samples isolated from subjects II and III, with 446 of them (60%) identified in the samples from both subjects. Combining the results from all experiments for the three subjects resulted in a total of 954 proteins after redundancy reduction. To our knowledge, the proteins reported here constitute the largest catalog of the healthy human skeletal muscle proteome to date. A detailed list of all proteins identified in this study together with their IPI ID, molecular weight, sequence coverage, and number of unique peptides assigned to each protein are provided as supplemental information (supplemental Table I). For each identified peptide sequence, we have included the following in supplemental Table II: modifications, flank residues, precursor mass, charge and mass error observed, the best Mascot score, and best peptide identification probability.

Among the proteins identified in this study, numerous entries derived from the protein identification searches had multiple IPI IDs. In many cases, assignment of multiple IDs results from the potential presence of protein isoforms, which cannot be distinguished on the basis of unique peptides. In our results tables, protein with multiple IDs were assigned to a "protein group" (supplemental Table I). Proteins that were attributed a unique IPI ID are listed as a single-entry protein group. As can be seen from supplemental Table I, by performing the analysis in this manner, there were 954 protein groups. Among them, the majority (562) had one IPI ID, 230 had two associated IPI IDs and 162 had more than two associated IPI IDs. For 354 of 392 protein groups containing two or more IPI IDs, the corresponding proteins are known to be translated from the same gene. For protein groups with multiple IPI IDs, the minimum, maximum, and mean of molecular weights (MW), and the number of amino acids in each protein sequence are listed in supplemental Table I.

The MW distribution of all 954 identified proteins is shown in Fig. 1*A*. Nearly one-third of the identified proteins have a MW within the range of 20–40 kDa, and more than two-thirds are below 60 kDa. Proteins ranged from 6.1 kDa (cardiac phospholamban) to 3823 kDa (titin). We found 11 proteins with a MW less than 10 kDa and 114 greater than 100 kDa. Thus, 13% of the identified proteins were outside of the typical separation limits of two-dimensional gel electrophoresis, which has optimum resolution in the 10–100 kDa range.

The subcellular location of 776 proteins could be assigned based on the Gene Ontology annotation information obtained from the UniProt database, while 178 remained unassigned (Fig. 1*B*). Fifty-nine percent of the identified proteins could be assigned to cytoplasm, representing the predominant subcellular location of all identified proteins in this study. It has been estimated that mitochondrial proteins comprise 4.8% of the total human proteome (33). However, in skeletal muscle, we found that 212 of the 954 proteins detected (22%) could be attributed to the mitochondrion. Nuclear proteins represented the third largest group, with 17% of all identified proteins.

Pathway Analysis

From the large number of proteins identified in our analyses, we decided to evaluate the potential applicability of this HPLC-ESI-MS/MS-based proteomic approach for quantitative assessment of skeletal muscle proteins in future studies aimed at elucidating the mechanism underlying changes in muscle structure and metabolism under different physiological and pathophysiological conditions. To do this, we examined the representation of the major metabolic pathways (glucose and lipid metabolism, electron transport, and oxidative phosphorylation), calcium homeostasis, myofibrillar apparatus, and components of IGF and insulin signaling among the proteins we identified.

Glucose and Lipid Metabolism

All enzymes involved in the glycolytic pathway, glycogen metabolism, and the citric acid cycle were identified in these experiments (Figs. 2*A–C*). Moreover, we identified several subunits of four kinases and one major phosphatase (PP1, serine/threonine-protein phosphatase) known to be involved in regulation of the phosphorylation of enzymes such as glycogen synthase or glycogen phosphorylase. In addition, the majority of proteins that are crucial for the activation and transport of fatty acids into the mitochondrion and subsequent degradation in the -oxidation pathway were identified (Fig. 2*D*). These include enzymes involved in the oxidation of long-chain, medium-chain and short-chain activated fatty acids as well as enzymes required for the oxidation of unsaturated fatty acids.

Electron Transport and Phosphorylation

The major role of electron transport complexes I–IV is transfer of electrons coupled with proton pumping, with the ultimate goal of enabling oxidative phosphorylation (OXPHOS), the final step in energy production. Many of the subunits that make up complexes I–V are embedded in the inner membrane of mitochondria and are, therefore, often more difficult to extract from their membrane environment. In our experiments, we identified 55 (Table I) of the 88 known subunits of these complexes (34, 35). Many of the subunits in complexes I–V are of low molecular weight, which may explain why a smaller number of these subunits was identified in our experiments using 10% gels [29 in experiment 1–1 and 20 in experiment 1–2 (subject I)] compared with the experiments using the gradient (4–20%) gels [41 in experiment 2–1 (subject II) and 51 in experiment 2–2 (subject III)]. Several mitochondrial carrier and transfer proteins were also identified in our analyses.

The phosphocreatine/creatine (PCr/Cr) pool is the major source of high energy phosphate bonds for ATP replenishment in skeletal muscle in response to energy-dependent activities such as muscle contraction. Regulation of this reservoir involves a number of enzymes, all of which were identified in this study (36). These enzymes included the catalytic -2 and the regulatory -1 subunits of AMPK kinase, two cytosolic isoforms of creatine kinase (M and B), the mitochondrial creatine kinase isoform, two adenylate kinase isoforms, ADP/ATP translocase, and three isoforms of porin (supplemental Table I). Together these enzymes have been suggested to comprise a PCr/Cr shuttle, which ensures an efficient mechanism by which PCr can be resynthesized by mitochondrial ATP synthesis (36).

Calcium Homeostasis

Calcium homeostasis and calcium-dependent signaling in skeletal muscle play major roles in a number of cellular processes such as contraction, apoptosis, the adiponectin-AMPK signaling pathway, insulin-mediated glucose uptake, and mitochondrial biogenesis and function (37–41). In the present study, we identified three members of the voltage-dependent calcium channel complex, the ryanodine receptor 1, calmodulin, and several important calcium/calmodulin binding or regulated proteins (Table II). These proteins

include two subunits of the phosphatase, calcineurin A, all four subunits of calcium/calmodulin dependent kinase II (CaMKII), cardiac phospholamban, and the two major calcium ATPases (SERCA1 and 2). We also identified a calcium-regulated receptor, T-cadherin, which has been suggested to be a potential adiponectin receptor (42), and the calcium binding protein, MO25, which is a member of the LKB1-STRADA-MO25 complex regulating phosphorylation of AMPK.

Insulin and IGF-I Signaling

Insulin and IGF-I have significant metabolic and growth promoting roles in skeletal muscle, and their respective signaling pathways are involved in skeletal muscle insulin resistance. Among the proteins currently believed to mediate the effect of insulin and IGF-I on glucose transport, glycogen synthesis, and protein synthesis in skeletal muscle (3–7, 43), we identified the glycogen-targeting subunit of PP1 (PP1g), several Rab proteins involved in GLUT4 translocation, and a number of eukaryotic translation initiation and elongation factors and ribosomal protein S6 kinase involved in protein synthesis (supplemental Table I). Moreover, a number of kinases, phosphatases and other proteins known to modulate insulin and IGF-I signaling (3) were found. In addition to those already mentioned, three subunits of another phosphatase, PP2A, MAP kinase, MAP kinase kinases, and serine/threonine kinases, were identified. A number of cytosolic and mitochondrial chaperones were also found. Of these, HSP90 and its co-chaperone cdc37, in particular, have been suggested to interact with PDK1 and Akt (44); both are elements of insulin and IGF-I signaling. Moreover, four isoforms of the phosphoserine/phosphothreonine binding 14–3-3 proteins were identified. They have been reported to bind to insulin receptor substrate (IRS)-1, IRS-2, and PDK1 and to modulate the activities of IRS-1 associated PI3-kinase and PDK1 (3).

Extracellular Matrix (ECM) and Contractile Proteins

Muscle adaptation in response to a number of physiological and pathophysiological conditions involves changes in ECM and contractile proteins (13, 14, 45). Among ECM proteins, we found three -subunits of type VI collagen, fibronectin, decorin, lumican, and prolargin. Multiple isoforms of proteins constituting the myofibrillar apparatus were identified, including four actin isoforms, three -actinin isoforms, nine myosin heavy chain isoforms, eight myosin light chains isoforms, two myomesin isoforms, and titin. Moreover, both slow and fast skeletal muscle isoforms of troponin I, C, and T in the troponin complex were identified together with several tropomyosin and tropomodulin isoforms.

Phosphorylation Sites

Although no attempt was made to enrich phosphopeptides, 35 phosphorylation sites in 24 proteins were detected with confidence (95% using Scaffold analysis, Table III). According to available databases (www.phosphosite.org, www.phospho.elm.eu.org, www.mitocheck.org, www.phosida.com and www.expasy.ch) and existing literature, 16 of these phosphorylation sites have been reported before, whereas 19 phosphorylation sites in 13 proteins appear to be novel. These new phosphorylation sites were identified on proteins critical for muscle metabolism such as aldolase A, alpha/beta-enolase, glyceraldehyde-3-phosphate dehydrogenase, creatine kinase M, and glycogen phosphorylase as well as on muscle-specific proteins such as myoglobin, myomesin 1, myosin binding protein C, and LIM domain-binding protein 3.

DISCUSSION

A number of previous proteomic studies of human skeletal muscle have been accomplished using protein separation by two-dimensional gel electrophoresis with subsequent

identification using MALDI-TOF/MS and/or HPLC-ESI-MS/MS analyses (18–23). Most are comparative studies reporting only proteins that are differentially regulated in conditions such as type 2 diabetes (23), obesity (22), Tibetans at high altitude (20), and aging (21), or in comparisons between different muscle fiber types (19). The proteins reported in those studies represent mainly highly abundant structural or metabolic proteins. Of the 62 different proteins reported in these five studies (19–23), 59 were also identified in the present investigation. In comparative experiments that employ two-dimensional gel electrophoresis, differences in spot staining intensity are used as a measure of changes in protein expression. However, since a large number of proteins are present in more than one differently migrating protein spot (due to the presence of different isoforms or post-translational modifications), it is difficult to get a reliable estimate of the total content of a specific protein by the two-dimensional gel approach (19, 23). Furthermore, those studies focus primarily on differentially regulated proteins; thus, many other proteins that are not altered in abundance or are present at too low a level to be easily quantified by spot analysis often are not identified.

In the past, there are only a limited number of reports in the literature on characterization of the human skeletal muscle proteome (18, 46). To date, the most comprehensive list of proteins of human vastus lateralis muscle has been reported by Gelfi *et al.* (18) who used two-dimensional gel electrophoresis, MALDI-TOF/MS, and HPLC-ESI-MS/MS. Approximately 500 protein spots were visualized by silver staining, and 150 spots were excised, resulting in identification of 107 different proteins. Of those 107 proteins, 101 were identified in the present study. In a more recent report using two-dimensional difference gel electrophoresis to characterize the effects of aging on the human skeletal muscle, ~2700 protein spots were visualized, 52 of which were differentially expressed, and 39 proteins were identified (21). However, in addition to difficulties in identifying proteins at the extremes of the MW and pI ranges, a major weakness in the two-dimensional gel approach is in detection and subsequent identification of low-abundance proteins. Moreover, identification of proteins in all spots detected in a two-dimensional gel, such as the 2700 reported by Gelfi *et al.* (21), would be extremely labor-intensive, even with robotic processing.

Nuclear extracts from human muscle specimens of unspecified origin obtained from surgery or autopsies have been analyzed by two-dimensional HPLC-ESI-MS/MS, resulting in the identification of 192 different muscle proteins (46). In our analysis of whole cell lysates of human vastus lateralis muscle, we identified 116 of these nuclear proteins. Among those we did not identify, half were either hypothetical proteins or were assigned to the mouse database.

For our analysis of the human muscle protein, we elected to apply a relatively simple approach based on one-dimensional gel electrophoresis and HPLC-ESI-MS/MS analysis, a strategy that has been successful in studies of human cell lines (28, 29) and can be used with very small amounts of tissue in clinical studies. Using this approach, we identified 954 different proteins, which to our knowledge, represents the most comprehensive identification of proteins in human vastus lateralis muscle. This list includes a large number of membraneassociated and low molecular weight proteins, indicating less issues in this regard compared with two-dimensional gel electrophoresis. In Fig. 1*B* is a comparison of the MW range of proteins identified in our study with those listed in the IPI human database. If the MW distribution of proteins in human muscle is the same as the in the human proteome catalogued in the IPI human database, we identified a lower than expected proportion of proteins under 20 kDa. This suggests that either there is a lack of detection of these proteins by our approach or else the molecular weights of proteins in human muscle do not parallel those of the entire proteome.

Mechanisms underlying changes in muscle structure and metabolism during different physiological and pathophysiological conditions have traditionally been studied by focusing on small numbers of genes or proteins. Transcriptional profiling has been applied to define the molecular signature of denervation, immobilization, exercise-training, age-related sarcopenia, insulin resistance and muscular dystrophy (8–15, 45). However, global profiling of temporal changes in metabolic enzymes and structural proteins and their posttranslational modifications in skeletal muscle *in vivo* has been limited by the lack of appropriate proteomic technology. The present study shows that it is feasible to obtain a comprehensive identification of human skeletal muscle proteins with full representation of enzymes involved in glucose and lipid metabolism, a high number of mitochondrial proteins, including 55 OXPHOS subunits and carrier/transport proteins involved in ATP synthesis, and multiple proteins involved in calcium homeostasis including calmodulin, CaMKII, phospholamban and calcineurin A, which have been shown to play a role in insulin-mediated glucose transport, mitochondrial biogenesis and transcriptional regulation of lipid oxidation genes (37–41). As expected, a diversity of isoforms of myofibrillar and cytoskeletal proteins was found, reflecting the mixed fiber type composition of the human vastus lateralis muscle. Of potential importance to future studies regarding insulin resistance, we were able to identify several kinases, phosphatases, and enzymes known to regulate glycogen synthase, glucose transport, and protein synthesis and to modulate proximal insulin and IGF-I signaling (3–7, 43). Moreover, 16 known and 19 previously unreported phosphorylation sites were detected without phosphopeptide enrichment.

An analysis of the activity and subunit composition of mitochondria plays a central role in the diagnosis of mitochondrial myopathies, the pathophysiology of type 2 diabetes and age-related sarcopenia, and physiological responses to exercise. In addition to the citric acid cycle, -oxidation and OXPHOS, mitochondrial proteins are involved in a variety of cellular processes, including intracellular calcium homeostasis, programmed cell death (apoptosis), and ion homeostasis. The 212 mitochondrial proteins identified in the present study represent, to our knowledge, the most comprehensive proteomic identification of mitochondrial proteins of human skeletal muscle reported to date. In a proteomic study of rat mitochondria purified from skeletal muscle, heart, and liver, 689 proteins were identified, with only small differences found between skeletal muscle and heart (47). The most extensive evaluation of human mitochondrial proteins identified 680 proteins in purified heart mitochondria (48), utilizing 40 mg of purified mitochondria as starting material and 701 HPLC-ESI-MS/MS analyses. Based on those results, it is likely that we would improve our coverage of the estimated 1500 human mitochondrial proteins (33) if muscle mitochondria were isolated prior to one-dimensional gel electrophoresis and HPLC-ESI-MS/MS. The finding that mitochondrial proteins accounted for 22% of all skeletal muscle proteins identified in the present study, compared with 4.8% in the total human proteome (33), may reflect the critical role that mitochondria play for energy metabolism in skeletal muscle and the enormous demand for ATP elicited by muscle contraction.

In conclusion, this study represents the first application of one-dimensional gel electrophoresis and HPLC-ESI-MS/MS for analysis of the human skeletal muscle proteome. Using only 60–70 μg of total protein from 3 lean subjects in <90 HPLC-ESI-MS/MS runs, we provide the most comprehensive proteome coverage of human skeletal muscle to date. This includes the largest catalog of mitochondrial proteins in human skeletal muscle. It is important to emphasize that the quantity of protein from each subject that was used in these experiments represents a small fraction of the muscle obtained by percutaneous needle biopsy. These data demonstrate the utility of this relatively simple proteomic approach for analysis of small human tissue samples, making it a potentially valuable tool in elucidating changes in the proteome associated with human disease.

Supplementary Material

Refer to Web version on PubMed Central for supplementary material.

REFERENCES

1. Bergstrom J. Percutaneous needle biopsy of skeletal muscle in physiological and clinical research. Scand. J. Clin. Lab. Invest. 1975; 35:609–616. [PubMed: 1108172]

2. Edwards R, Young A, Wiles M. Needle biopsy of skeletal muscle in the diagnosis of myopathy and the clinical study of muscle function and repair. N. Engl. J. Med. 1980; 302:261–271. [PubMed: 6985707]

3. Hojlund K, Beck-Nielsen H. Impaired glycogen synthase activity and mitochondrial dysfunction in skeletal muscle: markers or mediators in type 2 diabetes. Curr. Diabetes Rev. 2006; 2:375–395. [PubMed: 18220643]

4. Krebs M, Roden M. Molecular mechanisms of lipid-induced insulin resistance in muscle, liver and vasculature. Diabetes Obes. Metab. 2005; 7:621–632. [PubMed: 16219006]

5. Lowell BB, Shulman GI. Mitochondrial dysfunction and type 2 diabetes. Science. 2005; 307:384–387. [PubMed: 15662004]

6. Pirola L, Johnston AM, Van Obberghen E. Modulation of insulin action. Diabetologia. 2004; 47:170–184. [PubMed: 14722654]

7. Kelley DE, Mandarino LJ. Fuel selection in human skeletal muscle in insulin resistance: a reexamination. Diabetes. 2000; 49:677–683. [PubMed: 10905472]

8. Winokur ST, Chen YW, Masny PS, Martin JH, Ehmsen JT, Tapscott SJ, van der Maarel SM, Hayashi Y, Flanigan KM. Expression profiling of FSHD muscle supports a defect in specific stages of myogenic differentiation. Hum. Mol. Genet. 2003; 12:2895–2907. [PubMed: 14519683]

9. Giresi PG, Stevenson EJ, Theilhaber J, Koncarevic A, Parkington J, Fielding RA, Kandarian SC. Identification of a molecular signature of sarcopenia. Physiol. Genomics. 2005; 21:253–263. [PubMed: 15687482]

10. Patti ME, Butte AJ, Crunkhorn S, Cusi K, Berria R, Kashyap S, Miyazaki Y, Kohane I, Costello M, Saccone R, Landaker EJ, Goldfine AB, Mun E, DeFronzo R, Finlayson J, Kahn CR, Mandarino LJ. Coordinated reduction of genes of oxidative metabolism in humans with insulin resistance and diabetes: Potential role of PGC1 and NRF1. Proc. Natl. Acad. Sci. U. S. A. 2003; 100:8466–8471. [PubMed: 12832613]

11. Mootha VK, Lindgren CM, Eriksson KF, Subramanian A, Sihag S, Lehar J, Puigserver P, Carlsson E, Ridderstrale M, Laurila E, Houstis N, Daly MJ, Patterson N, Mesirov JP, Golub TR, Tamayo P, Spiegelman B, Lander ES, Hirschhorn JN, Altshuler D, Groop LC. PGC-1alpha-responsive genes involved in oxidative phosphorylation are coordinately downregulated in human diabetes. Nat. Genet. 2003; 34:267–273. [PubMed: 12808457]

12. Sreekumar R, Halvatsiotis P, Schimke JC, Nair KS. Gene expression profile in skeletal muscle of type 2 diabetes and the effect of insulin treatment. Diabetes. 2002; 51:1913–1920. [PubMed: 12031981]

13. Richardson DK, Kashyap S, Bajaj M, Cusi K, Mandarino SJ, Finlayson J, DeFronzo RA, Jenkinson CP, Mandarino LJ. Lipid infusion decreases the expression of nuclear encoded mitochondrial genes and increases the expression of extracellular matrix genes in human skeletal muscle. J. Biol. Chem. 2005; 280:10290–10297. [PubMed: 15598661]

14. Batt J, Bain J, Goncalves J, Michalski B, Plant P, Fahnestock M, Woodgett J. Differential gene expression profiling of short and long term denervated muscle. FASEB J. 2006; 20:115–117. [PubMed: 16291642]

15. Teran-Garcia M, Rankinen T, Koza RA, Rao DC, Bouchard C. Endurance training-induced changes in insulin sensitivity and gene expression. Am. J. Physiol. Endocrinol. Metab. 2005; 288:E1168–E1178. [PubMed: 15687108]

16. Anderson L, Seilhamer J. A comparison of selected mRNA and protein abundances in human liver. Electrophoresis. 1997; 18:533–537. [PubMed: 9150937]

17. Gygi SP, Rochon Y, Franza BR, Aebersold R. Correlation between protein and mRNA abundance in yeast. Mol. Cell. Biol. 1999; 19:1720–1730. [PubMed: 10022859]

18. Gelfi C, De Palma S, Cerretelli P, Begum S, Wait R. Two-dimensional protein map of human vastus lateralis muscle. Electrophoresis. 2003; 24:286–295. [PubMed: 12652600]

19. Capitanio D, Vigano A, Ricci E, Cerretelli P, Wait R, Gelfi C. Comparison of protein expression in human deltoideus and vastus lateralis muscles using two-dimensional gel electrophoresis. Proteomics. 2005; 5:2577–2586. [PubMed: 15931664]

20. Gelfi C, De Palma S, Ripamonti M, Eberini I, Wait R, Bajracharya A, Marconi C, Schneider A, Hoppeler H, Cerretelli P. New aspects of altitude adaptation in Tibetans: a proteomic approach. FASEB J. 2004; 18:612–614. [PubMed: 14734630]

21. Gelfi C, Vigano A, Ripamonti M, Pontoglio A, Begum S, Pellegrino MA, Grassi B, Bottinelli R, Wait R, Cerretelli P. The human muscle proteome in aging. J. Proteome Res. 2006; 5:1344–1353. [PubMed: 16739986]

22. Hittel DS, Hathout Y, Hoffman EP, Houmard JA. Proteome analysis of skeletal muscle from obese and morbidly obese women. Diabetes. 2005; 54:1283–1288. [PubMed: 15855311]

23. Hojlund K, Wrzesinski K, Larsen PM, Fey SJ, Roepstorff P, Handberg A, Dela F, Vinten J, McCormack JG, Reynet C, Beck-Nielsen H. Proteome analysis reveals phosphorylation of ATP synthase beta-subunit in human skeletal muscle and proteins with potential roles in type 2 diabetes. J. Biol. Chem. 2003; 278:10436–10442. [PubMed: 12531894]

24. Washburn MP, Wolters D, Yates JR 3rd. Large-scale analysis of the yeast proteome by multidimensional protein identification technology. Nat. Biotechnol. 2001; 19:242–247. [PubMed: 11231557]

25. Jacobs JM, Mottaz HM, Yu LR, Anderson DJ, Moore RJ, Chen WN, Auberry KJ, Strittmatter EF, Monroe ME, Thrall BD, Camp DG 2nd, Smith RD. Multidimensional proteome analysis of human mammary epithelial cells. J. Proteome Res. 2004; 3:68–75. [PubMed: 14998165]

26. Pan Y, Kislinger T, Gramolini AO, Zvaritch E, Kranias EG, MacLennan DH, Emili A. Identification of biochemical adaptations in hyper- or hypocontractile hearts from phospholamban mutant mice by expression proteomics. Proc. Natl. Acad. Sci. U. S. A. 2004; 101:2241–2246. [PubMed: 14982994]

27. Metz TO, Jacobs JM, Gritsenko MA, Fontes G, Qian WJ, Camp DG 2nd, Poitout V, Smith RD. Characterization of the human pancreatic islet proteome by two-dimensional LC/MS/MS. J. Proteome Res. 2006; 5:3345–3354. [PubMed: 17137336]

28. Schirle M, Heurtier MA, Kuster B. Profiling core proteomes of human cell lines by one-dimensional PAGE and liquid chromatography-tandem mass spectrometry. Mol. Cell. Proteomics. 2003; 2:1297–1305. [PubMed: 14532353]

29. Rezaul K, Wu L, Mayya V, Hwang SI, Han D. A systematic characterization of mitochondrial proteome from human T leukemia cells. Mol. Cell. Proteomics. 2005; 4:169–181. [PubMed: 15598749]

30. Lasonder E, Ishihama Y, Andersen JS, Vermunt AM, Pain A, Sauerwein RW, Eling WM, Hall N, Waters AP, Stunnenberg HG, Mann M. Analysis of the Plasmodium falciparum proteome by high-accuracy mass spectrometry. Nature. 2002; 419:537–542. [PubMed: 12368870]

31. Lowry OH, Rosebrough NJ, Farr AL, Randall RJ. Protein measurement with the Folin phenol reagent. J. Biol. Chem. 1951; 193:265–275. [PubMed: 14907713]

32. Foster LJ, Rudich A, Talior I, Patel N, Huang X, Furtado LM, Bilan PJ, Mann M, Klip A. Insulin-dependent interactions of proteins with GLUT4 revealed through stable isotope labeling by amino acids in cell culture (SILAC). J. Proteome Res. 2006; 5:64–75. [PubMed: 16396496]

33. Guda C, Fahy E, Subramaniam S. MITOPRED: a genome-scale method for prediction of nucleus-encoded mitochondrial proteins. Bioinformatics. 2004; 20:1785–1794. [PubMed: 15037509]

34. Carroll J, Fearnley IM, Skehel JM, Shannon RJ, Hirst J, Walker JE. Bovine complex I is a complex of 45 different subunits. J. Biol. Chem. 2006; 281:32724–32727. [PubMed: 16950771]

35. Scheffler, IE. The Human OXPHOS system: Structure, Function, Physiology. Landes Bioscience and Kluwer Academic/Plenum Publishers; 2004.

36. Neumann D, Schlattner U, Wallimann T. A molecular approach to the concerted action of kinases involved in energy homoeostasis. Biochem. Soc. Trans. 2003; 31:169–174. [PubMed: 12546678]

37. Gunter TE, Yule DI, Gunter KK, Eliseev RA, Salter JD. Calcium and mitochondria. FEBS Lett. 2004; 567:96–102. [PubMed: 15165900]

38. Konstantopoulos N, Marcuccio S, Kyi S, Stoichevska V, Castelli LA, Ward CW, Macaulay SL. A purine analog kinase inhibitor, calcium/calmodulin-dependent protein kinase II inhibitor 59, reveals a role for calcium/calmodulin-dependent protein kinase II in insulin-stimulated glucose transport. Endocrinology. 2007; 148:374–385. [PubMed: 17008397]

39. Lanner JT, Katz A, Tavi P, Sandstrom ME, Zhang SJ, Wretman C, James S, Fauconnier J, Lannergren J, Bruton JD, Westerblad H. The role of Ca2+ influx for insulin-mediated glucose uptake in skeletal muscle. Diabetes. 2006; 55:2077–2083. [PubMed: 16804078]

40. Long YC, Glund S, Garcia-Roves PM, Zierath JR. Calcineurin regulates skeletal muscle metabolism via coordinated changes in gene expression. J. Biol. Chem. 2007; 282:1607–1614. [PubMed: 17107952]

41. Wu H, Kanatous SB, Thurmond FA, Gallardo T, Isotani E, Bassel-Duby R, Williams RS. Regulation of mitochondrial biogenesis in skeletal muscle by CaMK. Science. 2002; 296:349–352. [PubMed: 11951046]

42. Hug C, Wang J, Ahmad NS, Bogan JS, Tsao TS, Lodish HF. T-cadherin is a receptor for hexameric and high-molecular-weight forms of Acrp30/adiponectin. Proc. Natl. Acad. Sci. U. S. A. 2004; 101:10308–10313. [PubMed: 15210937]

43. Solomon AM, Bouloux PM. Modifying muscle mass: the endocrine perspective. J. Endocrinol. 2006; 191:349–360. [PubMed: 17088404]

44. Basso AD, Solit DB, Chiosis G, Giri B, Tsichlis P, Rosen N. Akt forms an intracellular complex with heat shock protein 90 (Hsp90) and Cdc37 and is destabilized by inhibitors of Hsp90 function. J. Biol. Chem. 2002; 277:39858–39866. [PubMed: 12176997]

45. Urso ML, Scrimgeour AG, Chen YW, Thompson PD, Clarkson PM. Analysis of human skeletal muscle after 48 h immobilization reveals alterations in mRNA and protein for extracellular matrix components. J. Appl. Physiol. 2006; 101:1136–1148. [PubMed: 16763108]

46. Cagney G, Park S, Chung C, Tong B, O'Dushlaine C, Shields DC, Emili A. Human tissue profiling with multidimensional protein identification technology. J. Proteome Res. 2005; 4:1757–1767. [PubMed: 16212430]

47. Reifschneider NH, Goto S, Nakamoto H, Takahashi R, Sugawa M, Dencher NA, Krause F. Defining the mitochondrial proteomes from five rat organs in a physiologically significant context using two-dimensional blue-native/SDS-PAGE. J. Proteome Res. 2006; 5:1117–1132. [PubMed: 16674101]

48. Taylor SW, Fahy E, Zhang B, Glenn GM, Warnock DE, Wiley S, Murphy AN, Gaucher SP, Capaldi RA, Gibson BW, Ghosh SS. Characterization of the human heart mitochondrial proteome. Nat. Biotechnol. 2003; 21:281–286. [PubMed: 12592411]
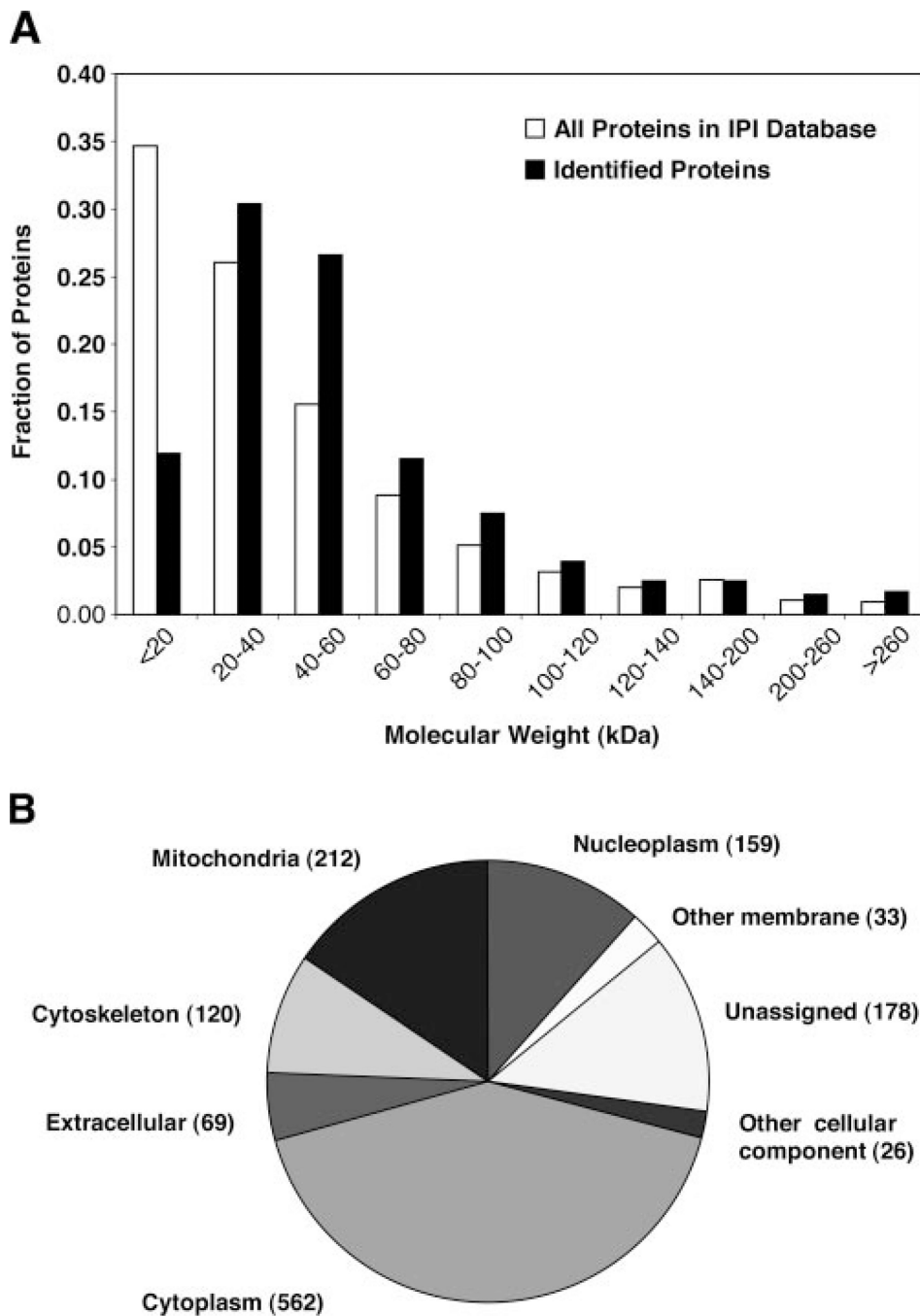
Fig. 1. Molecular weight distribution and subcellular location of human skeletal muscle proteins
A, distribution of the 954 proteins identified in human vastus lateralis muscle (*closed bars*) compared with all proteins in the IPI human database (*open bars*) relative to their predicted molecular weight. *B*, distribution of the 954 identified proteins according to Gene Ontology (GO) annotation. In cases where an identified protein group contained more than one IPI ID, the average molecular weight was used.

A Glycogen metabolism

Synthesis

Glucose-6-phosphate → Phosphoglucomutase 1 | PGM1 37 / 65%
Glucose-1-phosphate
UTP, PPi → UDP glucose pyrophosphorylase | UGP2 21 / 51%
UDP-glucose
Glycogen (n residues) → Glycogen synthase | GYS1 17 / 29%
UDP → Glycogen branching enzyme | GBE1 5 / 9%
Glycogen (n+1 residues)

Degradation

Glycogen (n residues)
PYGM 73 / 63% | Glycogen phosphorylase
AGL 46 / 35% | Glycogen debrancher
Glycogen (n-1 residues)
Glucose-1-phosphate
PGM1 37 / 65% | Phosphoglucomutase 1
Glucose-6-phosphate

Regulators of glycogen synthase or phosphoylase

CKII	CKI	GSK3	AMPK	CaMKII	PP1	PhK	PKA
			PRKAA2 5 / 13%	CAMK2A 4 / 13%	PPP1CB 4 / 17%	PHKA1 17 / 16%	PRKAR1A 11 / 32%
			PRKAG1 4 / 17%	CAMK2B 7 / 13%	PPP1R3A 2 / 2%	PHKB 11 / 12%	PRKAR2A 13 / 48%
				CAMK2D 5 / 15%			LOC730418 8 / 29%
				CAMK2G 5 / 13%			

B Glycolytic pathway

Glucose
ATP, ADP → Hexokinase | HK1 18 / 20%
Glucose-6-phosphate
Glucose-6-phosphate isomerase | GPI 24 / 47%
Fructose-6-phosphate
ATP, ADP → Phospho fructokinase 1 | PFKM 36 / 39%
Fructose-1,6-bisphosphate
Aldolase | ALDOA 38 / 71%
Dihydroxyacetone phosphate → Triosephosphate isomerase | TPI1 12 / 44%
Glyceraldehyde-3-dehydrogenase
NADH → Glyceraldehyde-3-phosphate dehydrogenase | GAPDH 32 / 69%
1,3-bisphosphoglycerate
ADP, ATP → Phosphoglycerate kinase | PGK1 29 / 64%
3-phosphoglycerate
Phosphoglycerate mutase | PGAM2 14 / 48%
2-phosphoglycerate
Enolase | ENO1 19 / 50% | ENO2 4 / 7% | ENO3 39 / 17%
phosphoenolpyruvate
ADP, ATP → Pyruvate kinase | PKM2 (1) 53 / 64% | PKM2 (2) 46 / 64%
pyruvate
LDHB 12 / 33% | LDHA 20 / 52% | Lactate dehydrogenase
Lactat

C Citric acid cycle

Pyryvate → Pyryvate dehydrogenase complex | PDHA1 14 / 35% | DLAT (1) 12 / 19% | DLAT (2) 7 / 13% | PDHB 10 / 32% | PDHX 11 / 30%
Acetyl Coa → Citrate
Citrate synthase | CS 14 / 32%
ACO2 37 / 47% | Aconitase
cis-Aconitate
ACO2 37 / 47% | Aconitase
Isocitrate
IDH3A 6 / 21% | IDH2 28 / 40% | IDH3G 4 / 21% | IDH3B 5 / 19% | Isocitrate dehydrogense
NADH
α-Keto-glutarate
OGDH 28 / 35% | DLST 11 / 25% | α-Ketoglutarate dehydrogenase complex
NADH
Succinyl CoA
SUCLA2 10 / 34% | SUCLG2 5 / 12% | SUCLG1 6 / 23% | Succinyl CoA synthetase
GTP
Succinate
SDHA 12 / 22% | SDHB 6 / 24% | Succinate dehydrogense | FADH2
Fumarate
FH 14 / 40% | Fumarase
Malate
MDH2 16 / 49% | Malate dehydrogense
NADH
Oxaloacetate

D Fatty acid transport and oxidation

Outer Mitochondrial Membrane / Cytoplasm

FFA
ATP, AMP → Acyl-CoA synthetase | ACSL1 19 / 30% | ACSL3 4 / 9%
Acyl CoA (long-chain)
Carnitine palmitoyl-transferase 1 | CPT1B 4 / 6%

Inner Mitochondrial Membrane

Acylcarnitine (long chain)
Carnitine palmitoyl-transferase 2 | CPTB2 8 / 18%
Acyl-CoA (long-chain)
FADH2 → Acyl-CoA dehydrogenase | ACADVL 30 / 42%
2-Enoyl-CoA (long-chain)
Trifunctional protein | HADHA 34 / 48% | HADHB 19 / 41%
Acyl-CoA (short & medium-chain)

Mitochondrial Matric

FADH2 → Acyl-CoA dehydrogenases | ACADM 11 / 35% | ACADS 10 / 35% | ACADSB 3 / 12%
NADP → 2,4-Dienoyl-CoA reductase + 3,2-trans-enoyl-CoA isomerase | DECR1 5 / 21% | DCI 4 / 15% | PECI 4 / 18% | ECH1 10 / 33%
2-Enoyl-CoA
2-Enoyl-CoA hydratases | ECHS1 5 / 19%
3-Hydroxyacyl-CoA
NADH → 3-Hydroxyacyl-CoA dehydrogenases | HADH 9 / 34% | HSD17B10 4 / 24%
3-Ketoacyl-CoA
3-Ketoacyl-CoA thiolases | ACAA2 11 / 39%
Acetyl-CoA

Fig. 2. Proteomics coverage of major enzymes involved in glucose and lipid metabolism in human skeletal muscle

A, isoforms and/or subunits of enzymes involved in glycogen metabolism. Glycolysis (*B*), citric acid cycle (*C*), and fatty acid transport (*D*) into and oxidation in mitochondria. Proteins identified are shown in *gray boxes*, and the associated gene names, maximum observed number of unique peptides, and sequence coverage are presented in adjacent *white boxes*.

Table I

Proteins involved in oxidative phosphorylation (OXPHOS) identified in human skeletal muscle

Proteins were separated by one-dimensional gel electrophoresis and identified by HPLC-ESI-MS/MS in four experiments using skeletal muscle from three nonobese, healthy subjects.

Protein	Gene name	MW (kDa)	Maximum unique peptides[a]	Maximum sequence coverage (%)[a]
Complex I				
NADH dehydrogenase 1 subunit C2	NDUFC2	14	2	17
NADH dehydrogenase 1 subcomplex subunit 2	NDUFA2	11	3	20
NADH dehydrogenase 1 subcomplex subunit 4	NDUFA4	9	2	22
NADH dehydrogenase 1 subcomplex subunit 5	NDUFA5	14	3	31
NADH dehydrogenase 1 subcomplex subunit 6	NDUFA6	18	2	12
NADH dehydrogenase 1 subcomplex subunit 7	NDUFA7	13	3	35
NADH dehydrogenase 1 subcomplex subunit 8	NDUFA8	20	3	30
NADH dehydrogenase 1 subcomplex subunit 9	NDUFA9	43	7	26
NADH dehydrogenase 1 subcomplex subunit 10	NDUFA10	41	6	16
NADH dehydrogenase 1 subcomplex subunit 12	NDUFA12	17	2	20
NADH dehydrogenase 1 subcomplex subunit 13	NDUFA13	26	4	22
NADH dehydrogenase 1 subcomplex subunit 3	NDUFB3	11	2	21
NADH dehydrogenase 1 subcomplex subunit 4	NDUFB4	15	2	17
NADH dehydrogenase 1 subcomplex subunit 5	NDUFB5	20	3	12
NADH dehydrogenase 1 subcomplex subunit 7	NDUFB7	16	2	12
NADH dehydrogenase 1 subcomplex subunit 8	NDUFB8	20	2	22
NADH dehydrogenase 1 subcomplex subunit 9	NDUFB9	21	3	27
NADH dehydrogenase 1 subcomplex subunit 10	NDUFB10	21	4	31
NADH dehydrogenase 1 subcomplex subunit 11 isoform 2	NDUFB11	18	2	21
NADH-ubiquinone oxidoreductase 9.6 kDa subunit	NDUFAB1	17	3	15
NADH-ubiquinone oxidoreductase 75 kDa subunit	NDUFS1	79	21	36
NADH dehydrogenase iron-sulfur protein 2	NDUFS2	53	15	45
NADH dehydrogenase iron-sulfur protein 3	NDUFS3	30	5	20
NADH dehydrogenase iron-sulfur protein 4	NDUFS4	20	2	15
NADH dehydrogenase iron-sulfur protein 5	NDUFS5	12	3	25
NADH dehydrogenase iron-sulfur protein 7	NDUFS7	28	3	15
NADH dehydrogenase iron-sulfur protein 8	NDUFS8	24	3	15
NADH dehydrogenase flavoprotein 1 isoform 1	NDUFV1	50	12	24
NADH dehydrogenase flavoprotein 2	NDUFV2	26	2	11
NADH dehydrogenase flavoprotein 3	NDUFV3	51	2	7
Complex II				
Succinate dehydrogenase flavoprotein subunit	SDHA	73	12	22
Succinate dehydrogenase iron-sulfur protein	SDHB	32	6	24
Complex III				

Protein	Gene name	MW (kDa)	Maximum unique peptides[a]	Maximum sequence coverage (%)[a]
Ubiquinol-cytochrome c reductase iron-sulfur subunit	UQCRFS1	30	5	22
Cytochrome c1, heme protein	CYC1	35	5	16
Ubiquinol-cytochrome-c reductase complex core protein I	UQCRC1	53	11	28
Ubiquinol-cytochrome-c reductase complex core protein 2	UQCRC2	48	13	41
Ubiquinol-cytochrome c reductase complex 14 kDa protein	UQCRB	13	3	32
Ubiquinol-cytochrome c reductase complex 7.2 kDa protein	UCRC	7	2	38
Complex IV				
Cytochrome c oxidase subunit 2	COX2	26	6	39
Cytochrome c oxidase subunit 4 isoform 1	COX4I1	20	8	46
Cytochrome c oxidase subunit 5A	COX5A	17	3	25
Cytochrome c oxidase subunit 5B	COX5B	14	2	9
Cytochrome c oxidase polypeptide Vic	COX6C	9	5	37
Cytochrome c oxidase polypeptide VIIa-Heart	COX7A1	11	2	29
Complex V				
ATP synthase B chain	ATP5F1	26	9	36
ATP synthase D chain isoform 1	ATP5H	18	9	52
ATP synthase E chain	ATP5I	8	3	50
ATP synthase F chain isoform 2	ATP5J2	8	2	44
ATP synthase subunit G	ATP5L	11	7	54
ATP synthase subunit	ATP5A1	60	39	62
ATP synthase subunit	ATP5B	57	40	75
ATP synthase chain	ATP5D	17	3	23
ATP synthase chain isoform heart	ATP5C1	33	5	18
ATP synthase coupling factor 6	ATP5J	13	5	45
ATP synthase O subunit (OSCP)	ATP5O	23	6	35
Carrier/transfer proteins				
Cytochrome c	CYCS	12	6	50
Phosphate carrier protein isoform A	SLC25A3	35	4	12
ADP/ATP translocase 1	SLC25A4	33	10	35
Mitochondrial 2-oxoglutarate/malate carrier protein	SLC25A11	34	7	26
Calcium-binding mitochondrial carrier protein Aralar1	SLC25A12	75	28	52
Electron transfer flavoprotein subunit	ETFA	35	6	27
Electron transfer flavoprotein subunit	ETFB	33	9	33
Electron transfer flavoprotein-ubiquinone oxidoreductase	ETFDH	68	9	20
NAD(P) transhydrogenase	NNT	114	11	14

MW, molecular weight; the mean molecular weight is shown for proteins with more than one IPI ID.

[a] Maximum values for one analysis.

Table II
Proteins involved in calcium homeostasis identified in human skeletal muscle

Proteins were separated by one-dimensional gel electrophoresis and identified by HPLC-ESI-MS/MS in four experiments using skeletal muscle from three nonobese, healthy subjects.

Protein	Gene name	MW (kDa)	Maximum unique peptides[a]	Maximum sequence coverage (%)[a]
Calcium Channels/Receptors				
Dihydropyridine receptor 2	CACNA2D1	125	10	13
Voltage-dependent L-type calcium channel -S1	CACNA1S	212	2	2
Voltage-dependent L-type calcium channel -1	CACNB1	64	9	23
Ryanodine receptor 1	RYR1	565	8	3
Calcium-Adiponectin-AMPK				
Cadherin 13 (T-cadherin)	CDH13	78	4	8
5 -AMP-activated protein kinase catalytic -2	PRKAA2	62	5	13
5 -AMP-activated protein kinase regulatory -1	PRKAG1	38	4	17
Calcium-binding protein 39 (Protein Mo25)	CAB39	40	6	18
Calcium regulated enzymes				
Calmodulin	CALM1	17	4	42
Calmodulin-dependent calcineurin A	PPP3CA	58	3	8
Calmodulin-dependent calcineurin A	PPP3CB	58	4	10
Calcium/calmodulin-dependent protein kinase II	CAMK2A	54	4	13
Calcium/calmodulin-dependent protein kinase II	CAMK2B	73	7	13
Calcium/calmodulin-dependent protein kinase II	CAMK2D	56	5	15
Calcium/calmodulin-dependent protein kinase II	CAMK2G	59	5	13
Cardiac phospholamban	PLN	6	3	23
Sarcoplasmic/endoplasmic reticulum calcium ATPase 1	ATP2A1	103	41	36
Sarcoplasmic/endoplasmic reticulum calcium ATPase 2	ATP2A2	110	42	33
GTP-binding protein RAD	RRAD	33	2	10
Calpain-1 catalytic subunit	CAPN1	82	12	22
Calpain-2 catalytic subunit	CAPN2	80	3	5
Calpain-3	CAPN3	94	7	13
Calpain small subunit 1	CAPNS1	31	4	18
Calcium binding proteins				
Calreticulin	CALR	42	2	9
Calnexin	CANX	68	5	11
Sarcalumenin	SRL	97	20	26
Sarcoplasmic reticulum histidine-rich calcium-binding protein	HRC	81	4	12
Calsequestrin-1	CASQ1	45	15	28
Calsequestrin-2	CASQ2	46	10	29
Annexin A1	ANXA1	39	7	28
Annexin A2	ANXA2	40	15	48
Annexin A4	ANXA4	35	2	8

Protein	Gene name	MW (kDa)	Maximum unique peptides[a]	Maximum sequence coverage (%)[a]
Annexin A5	ANXA5	36	14	42
Annexin A6	ANXA6	76	32	53
Annexin A7	ANXA7	52	4	11
Annexin A11	ANXA11	54	8	22
S-100 calcium-binding protein A1	S-100A1	11	2	38
S-100 calcium-binding protein A6	S-100A6	10	2	17
Copine-3	CPNE3	60	3	7
Gelsolin	GSN	83	12	25

MW, molecular weight; the mean molecular weight is shown for proteins with more than one IPI ID.

[a] Maximum values for one analysis.

<div align="center">

Table III

Phosphorylation sites in human skeletal muscle proteins identified by HPLC-ESI-MS/MS

</div>

Proteins were separated by one-dimensional gel electrophoresis and phosphorylation sites were identified by HPLC-ESI-MS/MS in four experiments using skeletal muscle from three nonobese, healthy subjects. No phosphopeptide enrichment strategies were used.

Protein	Gene name	Sequence[a]	Mono-phosphorylation site(s)
Aldolase A	ALDOA	^{29}GILAADESTGSIAK^{42}	S36, T37,[b] S39
Alpha crystallin family protein	CRYAB	^{29}RASAPLPGLSAPGR^{42}	S31
Alpha/beta-enolase	ENO1/3	^{33}AAVPSGASTGIYEALELR^{50}	S40,[b] T41,[b] Y44
cAMP-dependent protein kinase regulatory −1 subunit	PRKAR2A	^{75}TDSREDEISPPPPNPVVK^{92}	S83
Carbonic anhydrase 3	CA3	^{40}HDPSLQPWSVSYDGGSAK^{57}	S48[b]
Cardiac phospholamban	PLN	^{14}RASTIEMPQQAR^{25}	S16
Cardiac phospholamban	PLN	^{14}ASTIEMPQQAR^{25}	T17
Creatine kinase M	CKM	^{157}LSVEALNSLTGEFK^{170}	S164[b]
Creatine kinase M	CKM	^{321}GTGGVDTAAVGSVFDVSNADR^{341}	T322,[b] T327,[b] S332[b]
Gamma filamin variant	FLNC	^{2211}LGSFGSITR^{2219}	S2213
Glyceraldehyde-3-phosphate dehydrogenase	GAPDH	^{163}VIHDNFGIVEGLMTTVHAITATQK^{186}	T182, T184[b]
Glycogen phosphorylase, muscle form	PYGM	^{467}TIFKDFYELEPHK^{479}	Y473[b]
Glycogen synthase, muscle	GYS1	^{708}RNSVDTATSSSLSTPSEPLSPTSSLGEERN^{737}	S710
Heat-shock protein beta-1	HSPB1	^{80}QLSSGVSEIR^{89}	S82
Phosphorylase B kinase regulatory subunit	PHKA1	^{972}SVRPTDSNVSPAISIHEIGAVGATK^{996}	S972
LIM domain-binding protein 3	LDB3	^{189}DLAVDSASPVYQAVIK^{204}	Y199[b]
MYC box-dependent-interacting protein 1	BIN1	^{296}SPSPPDGSPAATPEIR^{311}	S298
Myoglobin	MB	^{65}HGATVLTALGGILK^{78}	T68,[b] T71[b]
Myomesin 1	MYOM1	^{63}RASASSSQQQASQHALSSEVSR^{84}	S65[b]
Myosin binding protein C, slow type	MYBPC1	^{57}KDSDWTLVETPPGEEQAK^{74}	S59[b]
Myosin binding protein C, fast type	MYBPC2	^{37}EAPPEDQSPTAEEPTGVFLK^{56}	S44[b]
Pyruvate dehydrogenase, E1 component subunit	PDHA1	^{289}YHGHSMSDPGVSYR^{302}	Y289, T293
RAS GTPase-activating protein-binding protein 1	G3BP1	^{230}SSSPAPADIAQTVQEDLR^{247}	S232
Sarcoplasmic reticulum His-rich calcium-binding protein	HRC	^{113}VGDEGVSGEEVFAEHGGQAR^{132}	S119[b]
Sarcoplasmic reticulum His-rich calcium-binding protein	HRC	^{157}SHSHQDEDEDEVVSSEHHHHILR^{179}	S170[b]
Smoothelin-like 2	SMTNL2	^{342}SQSFGVASASSIK^{354}	S344[b]

[a] The sequence location of each peptide is indicated in superscript.

[b] Sites that appear to be novel.